Supervised Learning-Assisted Modeling of Flow-Based Domains in European Resource Adequacy Assessments

Zad, Bashir Bakhshideh; Toubeau, Jean-François ; Bruninx, K.; Vatadoust, Behzad; De Grève, Zacharie; Vallée, François

DOI
10.1016/j.apenergy.2022.119875

Publication date
2022

Document Version
Final published version

Published in
Applied Energy

Citation (APA)
Zad, B. B., Toubeau, J.-F., Bruninx, K., Vatadoust, B., De Grève, Z., & Vallée, F. (2022). Supervised Learning-Assisted Modeling of Flow-Based Domains in European Resource Adequacy Assessments. *Applied Energy*, *325*, Article 119875. https://doi.org/10.1016/j.apenergy.2022.119875

Applied Energy 325 (2022) 119875

Contents lists available at ScienceDirect

Applied Energy

journal homepage: www.elsevier.com/locate/apenergy

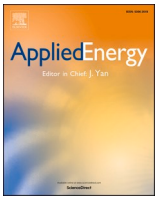

Supervised learning-assisted modeling of flow-based domains in European resource adequacy assessments

Bashir Bakhshideh Zad [a,*], Jean-François Toubeau [a], Kenneth Bruninx [b,c,d], Behzad Vatandoust [a], Zacharie De Grève [a], François Vallée [a]

[a] Power Systems and Markets Research Group, University of Mons, Belgium
[b] Faculty of Technology, Policy and Management, Delft University of Technology, the Netherlands
[c] Energy Systems Integration and Modeling Group, University of Leuven, Belgium
[d] EnergyVille, Belgium

HIGHLIGHTS

- This paper aims to enhance the modeling of cross-border energy exchanges in adequacy study.
- Novel supervised learning-based models in single- and two-step set-ups are proposed.
- Accuracy, scalability, and computational complexity of adequacy study are improved.
- It can have high implication for policy makers and be of a great interest of academics.

ARTICLE INFO

Keywords:
Adequacy assessments
Flow-based market coupling
Cross-border exchanges
Supervised learning
Unsupervised learning
Correlation study

ABSTRACT

To represent the cross-border exchange capacities defined by the flow-based approach in the European resource adequacy assessments, transmission system operators currently employ a data-driven methodology that consists of sequential clustering and correlation steps. This methodology entails assumptions and simplifications within both clustering and correlation analyses that may lead to an erroneous representation of import–export capacities in the subsequent adequacy assessments. While the first stage of this methodology can be improved by leveraging a clustering technique tailored to adequacy assessments, the correlation step presents a poor performance in terms of accuracy and scalability. To address the latter challenges, this paper proposes a supervised learning-based model that can enhance the mapping between several relevant explanatory variables and the pre-clustered flow-based domains, leading to a more accurate representation of the flow-based domains in adequacy assessments. Furthermore, the current paper leverages supervised learning to develop a single-step approach that directly maps the selected explanatory variables to the flow-based domains using the K-Nearest Neighbors algorithm, eliminating the clustering step. This circumvents inaccuracies introduced by the significant intra-cluster discrepancies due to numerous shapes and forms of the flow-based domains and enables an enhanced modeling of the flow-based domains in adequacy assessments. In an extensive case study, we demonstrate that the proposed single-step model can significantly improve the accuracy of adequacy assessments, compared to the best-in-class result obtained by the two-step set-up. Moreover, the proposed single-step model involves no hyper-parameters, eliminates the computational complexity of the two-step set-up, and efficiently upscales to integrate the new zones joining to the flow-based market coupling.

1. Introduction

A resource adequacy study assesses the ability of an electric power system to meet the load demand over the future horizon under various working conditions. Such an assessment can be carried out in a deterministic or probabilistic manner. While the former category considers the peak load demand and available generation to evaluate the capacity (or deficit) margin, the latter generally takes advantage of Monte Carlo simulations that permit to capture the uncertain nature of load and

* Corresponding author.
E-mail address: bashir.bakhshidehzad@umons.ac.be (B. Bakhshideh Zad).

https://doi.org/10.1016/j.apenergy.2022.119875
Received 1 April 2022; Received in revised form 1 August 2022; Accepted 16 August 2022
Available online 29 August 2022

Nomenclature

Acronyms:

CWE	Central Western Europe
ENS	Energy Not Served
FB	Flow-Based
FBMC	Flow-Based Market Coupling
GO	Goal-Oriented
PTDF	Power Transfer Distribution Factor
RAM	Remaining Available Margin
TENS	Total Energy Not Served
TSO	Transmission System Operator
KNN	K-Nearest Neighbors
RF	Random Forest
SB	Shape-Based
SVM	Support Vector Machine
LOLP	Loss of Load Probability
PP	Percentage Point
MC	Monte Carlo

Indices and sets:

$p \in P$	Index and set for the time steps of the training phase
$q \in Q$	Index and set for the time steps of the test phase
$t \in T$	Index and set for the time steps of the whole database
$z \in Z$	Index and set for the K observations nearest to the test observation x_q
$a \in A$	Index and set for the vertices of the flow-based domain A
$b \in B$	Index and set for the vertices of the flow-based domain B
i	Index representing a zone in the interconnected CWE electricity system

Parameters:

N	Number of zones in the interconnected CWE electricity system (= 5)
LD_i	Aggregated load demand in zone i
NP_i	Net position of zone i
G_i^{max}	Maximum available generation in zone i
$PTDF$	Power transfer distribution factor matrix
NP	Vector of zonal net positions
RAM	Vector of remaining (free) available margin (capacity) on the selected grid elements
Δ_{LOLP}	LOLP error between the true adequacy outcomes and the results of the studied test case
Δ_{TENS}	TENS error between the true adequacy outcomes and the results of the studied test case
$LOLP_i^{TC}$	LOLP index in zone i in the test case
$LOLP_i^{Ref}$	LOLP index in zone i in the reference case
$TENS_i^{TC}$	TENS in zone i in the test case
$TENS_i^{Ref}$	TENS in zone i in the reference case
x	Explanatory variables i.e., inputs of the supervised learning task
y	True output of the supervised learning task
$\hat{y}$	Predicted output of the supervised learning task
f_θ	Function representing the mapping between input and output spaces
L	Loss function of the classification problem
$I(y_z = j)$	Indicator variable that equals 1 if observation z belongs to class j, and 0 if $y_z \neq j$
$PR(\bullet)$	Conditional probability
k	Number of folds within the k-fold method (= 5)
K	Number of neighbors considered in the KNN algorithm
K_C	Number of classes in the classification task
C	Hyper-parameter defining the total cost of relaxing the hyperplane constraint in the SVM method
l_p	Total number of the training observations
n	Number of clusters
d_{SB}	Distance (dissimilarity) between two flow-based domains using the shape-based measure

Variables:

ENS_i	Energy not served in zone i
G_i	Aggregated generation in zone i
θ	Supervised learning variables to be optimized
$\beta_0, \beta_1, \beta_D, \epsilon_1, \epsilon_{lp}$	SVM variables to be optimized
M	Width of the margin in the SVM method

generation. Sequential and non-sequential Monte Carlo methods for adequacy assessments have been studied in [1–3,36].

In an interconnected electric power network, the cross-border exchange capacities constitute important inputs of any adequacy study [4]. Within the context of probabilistic adequacy assessment, Monte Carlo simulations aim at reflecting day-to-day operation of the studied power system. The cross-border capacities, therefore, can be incorporated into adequacy assessment by adopting the capacity calculation method employed in the operation stage of the power system. The Flow-Based (FB) approach is the target capacity calculation model to incorporate the interconnection exchanges into the Europe's internal electricity system [5]. The Flow-Based Market Coupling (FBMC) was initially implemented in 2015 in 4 Central Western Europe (CWE) zones. It will be extended to 13 countries (CORE region) in 2022. A FB domain considers the available capacity on the selected critical grid elements in a zonal fashion. It constitutes a polytope whose vertices define the possible zonal exchanges.

Reference [6] discusses how a FB domain is constructed considering the network model, input data, and parameter settings. The impacts of the internal (discretionary) parameters of the FB model on the FBMC outcomes are investigated in [7–10], which demonstrate how an optimal setting of such parameters can maximize the performance of the FBMC. In addition, a new method is proposed in [11] that aims to enhance the overall efficiency of the FBMC and its eventual remedial actions. Although the literature relating to the FBMC has been growing in recent years, the research on the modeling of FB domains in an adequacy assessment context is scarce.

Nevertheless, following the implementation of the FBMC in the CWE region, the European regulations mandate that the national or European resource adequacy assessment shall take into account the FB approach, where applicable [12]. To integrate the cross-border exchange capacities defined by the FB domains into the probabilistic adequacy assessments, the main challenge consists in finding the FB domain that correctly represents the potentially binding grid constraints for the system conditions at hand. Indeed, the hourly FB domains depend on the network operating points as well as the internal (discretionary) parameters of the FB model (e.g., generation shift keys for nodal to zonal conversion [7], the minimum threshold for selection of the critical network elements [8], and the minimum branch capacities reserved for the power exchanges [9–10]). A direct model-based calculation of hourly FB domains first necessitates adopting assumptions on the abovementioned parameters that are partly known to a Transmission System Operator (TSO) as the FB calculation entails a sequential process that relies on the exchange of data among the involved TSOs. Furthermore, conducting such a calculation process for each Monte Carlo sample noticeably increases the computational complexity of the

probabilistic adequacy study as it requires integrating the FB calculation process into the adequacy evaluation context.

Given the difficulties in the direct computation of FB domains, several European TSOs employ a data-driven alternative to integrate the cross-border capacities into adequacy assessments [13–18]. This employed methodology consists of two main steps. First, the historical FB domains are clustered based on their overall geometrical shapes into a reduced number of groups. Then, the obtained FB domain clusters are correlated with two selected explanatory variables affecting the FB domains. This two-step clustering-correlation methodology (described in Section 2.2) permits to define for each new Monte Carlo sample of the probabilistic adequacy study, its corresponding (FB domain) cluster representative. The above methodology, however, entails inefficiencies in both its clustering and correlation steps since a FB cluster prototype may poorly represent its intra-cluster FB domains, and the correlation study may fail to accurately define the relationship between the clustered FB domains and the selected explanatory variables. Consequently, the two-step methodology employed by the TSOs would lead to approximations in subsequent adequacy assessments.

Following the two-step framework developed by the TSOs to integrate the FB domains into adequacy assessments, the authors of the current work proposed a Goal-Oriented (GO) distance measure in [19], which can offer a tailored dissimilarity calculation and clustering of the FB domains for the subsequent adequacy assessments. The GO distance measure focuses on the vertices of FB domain that are decisive in an adequacy assessment context rather than considering the overall shapes of FB domains (polytopes) that are complex and multi-dimensional consisting of several hundred vertices. The adequacy analyses conducted in [19] demonstrate the improved accuracy, suitable scalability, and reduced time complexity of the GO clustering approach, compared to the clustering method employed by the TSOs that is based on the overall shapes of FB domains. Nevertheless, the second part of the methodology employed by the TSOs (i.e., the correlation study), not addressed in [19], still needs to be improved since it poorly performs in terms of accuracy and scalability (as discussed in Section 3).

In the present paper, we firstly propose a novel supervised learning-based model to enhance the mapping between several relevant explanatory variables (i.e., aggregated load demand and generation in each CWE zone) and the pre-clustered FB domains within the two-step set-up, improving (replacing) the correlation step. This supervised learning task is formulated as a classification study that aims at defining the correct class (FB domain cluster) based on the received explanatory variables. The proposed classification-based model presents two main advantages over the classical correlation study used by the TSOs. First, it does not need any initial feature scaling or discretization of the selected explanatory (input) variables (that can be seen as hyper-parameters affecting the outcomes of the study). Second, it is highly scalable to the number of explanatory variables received as input, which is essential to fully explore the complex relations present between the input–output spaces. The performance of the proposed supervised learning-based framework is evaluated using three classification algorithms, namely Random Forest (RF), K-Nearest Neighbors (KNN), and Support Vector Machine (SVM), which have different working principles and generalization capabilities to reveal the potentials of the proposed model.

Although the proposed supervised learning-based approach applied to the pre-clustered FB data can enhance the accuracy and scalability of the FB domain assignment task within the two-step framework, the intra-cluster discrepancies may remain significant that induce inevitable modeling inaccuracies in subsequent adequacy studies. To tackle this issue, in the current paper, we propose an alternative strategy that leverages supervised learning to develop a single-step model that directly maps the selected explanatory variables to FB domains, without doing a clustering analysis. This circumvents inaccuracies introduced by the significant intra-cluster discrepancies due to numerous shapes and forms of FB domains and leads to an enhanced modeling of FB domains in adequacy assessments. This single-step model takes advantage of the KNN algorithm and identifies the most similar FB domain (historically observed) to each new unseen sample of probabilistic adequacy assessments. The extensive simulations and analyses conducted in this paper confirm the superior performance of the single-step model in terms of modeling accuracy and time complexity.

In summary, the main contributions of the current paper are threefold:

First, we propose a novel supervised learning-based model to improve the mapping between several selected explanatory variables (i.e., aggregated load demand and generation in each CWE country) and the FB domain clusters within the two-step frame. By covering the shortcomings of the correlation study (discussed in Section 3) employed by the TSOs, the proposed model can lead to more realistic and accurate adequacy outcomes while being scalable with respect to the ongoing geographical extension of the FBMC (i.e., joining new market zones) that requires integrating additional explanatory variables.

Second, we suggest an innovative alternative approach, leveraging the supervised learning to integrate the FB domains into probabilistic adequacy assessments. The proposed single-step model directly maps the selected explanatory variables to the historical FB domains, without performing the clustering analysis. By capturing the temporal similarities contained in the FB database, this direct approach can enhance the modeling of the interconnection capacities in adequacy assessments resulting in more accurate outcomes, while the removal of the clustering step permits to considerably reduce the computational complexity of the FB domain assignment task such that the latter can be performed in a nearly real-time fashion.

Third, relying on the real FB database from [20], we assess the performance of the single-step model in comparison with eleven different set-ups of the two-step frame (based on the goal-oriented or shape-based clustering analysis combined with the correlation or classification study). This extensive case study and the detailed analysis (relying on the cross-validation technique) can thoroughly reveal the advantages and drawbacks of each studied model (summarized in Table 7) to eventually define the most efficient approach for the FB domains modeling.

The current paper showcases how a tailored supervised learning model can enhance accuracy, scalability, and computational complexity of the European resource adequacy assessments. As such, it complements the recent research on machine learning facilitating secure and cost-efficient management of power systems as reviewed in [21] and studied on different use cases such as optimal power flow [22,23], unit commitment [24], voltage control [39] and forecast [25] as well as system stability [26] and reliability [27,28].

The remainder of this paper is structured as follows. Section 2 briefly introduces the cross-border capacity modeling via the FB approach and presents the classical methodology employed by the CWE TSOs to incorporate the FB domains into the adequacy assessments. The proposed supervised learning-based model for enhancing the performance of the correlation analysis within the two-step frame is described in Section 3. The proposed single-step model that directly performs the FB domain assignment task is presented in Section 4. The validation framework to examine the performance of the studied methods is introduced in Section 5. The simulation results are given in Section 6, followed by the relevant discussions in Section 7 and conclusion in Section 8.

2. Adequacy assessment incorporating the flow-based domains

A FB domain represented by a system of linear constraints (introduced below) is integrated into the adequacy assessment by adding its corresponding linear constraints to the optimization problem that is at the core of the adequacy study. The CWE TSOs generally employ the Antares simulator [29] to perform the probabilistic adequacy assessments on the Monte Carlo scenarios defined by the latter tool.

2.1. Interconnection capacities modelled with the flow-based domains

Within the FB approach, the feasible cross-zonal exchanges are calculated by linearly approximating the physical grid constraints. This approximation aims at reflecting the impact of zonal power changes on the flows on (selected) critical network elements. The above analysis is performed on the studied power network model considering the so-called base case that represents the best estimate (forecast) of the network operating conditions at the studied horizon. In the context of the day-ahead network scheduling, the base case corresponds to the 2 days ahead forecasts of the studied electricity system. The physically allowed power flows for the cross-zonal exchanges are determined in the FB approach according to a set of linear constraints, presented below.

$$PTDF \times NP \leq RAM \tag{1}$$

where the PTDF (Power Transfer Distribution Factor) matrix represents the power flow variations in the selected network elements because of zonal net position changes. The net position of each zone (=export − import) is denoted by the NP vector. The RAM (Remaining Available Margin) vector gives the free (available) capacity on the (selected) grid elements for the cross-zonal exchanges. Equation (1) expresses that the zonal net position changes should not violate the available capacities on the selected grid elements (obtained in the base case analyses).

A FB domain at a given hour corresponds to the intersection of all half-spaces created by the system of linear constraints (1), which constructs a N-dimensional polytope (N denoting the number of zones involved in the FBMC). Reference [6] details how the components and parameters of the FB model are determined and discusses their eventual impacts on the FBMC outcome.

A FB domain is computed with respect to a set of given input parameters including the network working conditions (load demands and available generations) as well as the discretionary parameters of the FB approach (introduced in Section 1). Depending on the above parameters, the hourly FB domains take various shapes, forms, and sizes, such that the differences between feasible hourly zonal exchanges within a typical day can reach several gigawatts (GW) as demonstrated in Fig. 1. Such a wide range of variations in the cross-border exchange capacities can highly affect the adequacy assessment outcomes. Therefore, a realistic and accurate adequacy evaluation requires defining the FB domain (PTDF and RAM parameters) that correctly aligns with each generated Monte Carlo scenario of the probabilistic adequacy study.

2.2. Classical methodology employed by the TSOs (shape-based clustering-correlation)

A direct model-based calculation of FB domain for each scenario of the Monte Carlo analysis is not conceivable, as explained in Section 1. To integrate the FB domains into European resource adequacy assessments,

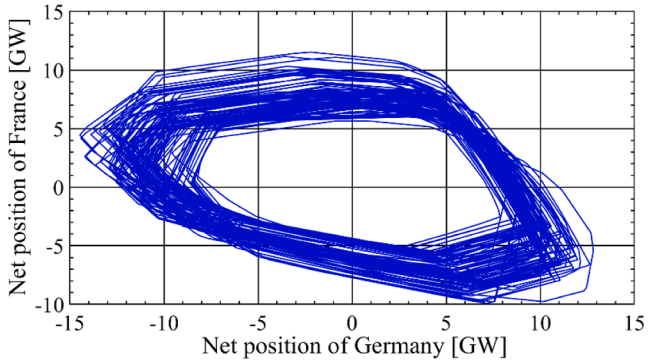

Fig. 1. Illustration of 96 hourly FB domains corresponding to 4 randomly selected days in January 2020, projected onto the France-Germany plane (data Source: [20]).

several European TSOs employ a two-step data-driven approach that consists of clustering and correlation analyses on the historical FB domains [13–18]. Fig. 2 demonstrates an overview of this two-step methodology employed by the TSOs. As it can be seen, the correlation model is trained with the historical data to identify the relation between the selected explanatory variables and the clustered FB domains. Within the adequacy evaluation context, the trained correlation model can determine the FB cluster representative that can better match with each Monte Carlo sample based on the received unseen explanatory variables. The two-step clustering-correlation methodology is summarized as follows.

1) Shape-Based (SB) clustering: The objective of the first step of the methodology is to group the historical FB domains into a limited number of clusters. A partitional clustering algorithm is employed to that end, in combination with a dissimilarity (or distance) measure, which compares the geometrical shapes of the FB domains. The distance (dissimilarity) between two FB domains is computed considering the coordinates of their polytope vertices. Let A and B be two sets, with $A = \{a_1, a_2, \cdots, a_n\}$ and $B = \{b_1, b_2, \cdots, b_m\}$, which present the N-dimensional vertices of the two selected FB domain polytopes. The dissimilarity between the FB domain A and FB domain B is calculated as follows using the Shape-Based (SB) measure.

$$d_{SB}(FB_A, FB_B) = \sum_{a \in A} \min_{b \in B} \sqrt{(a-b)^2} \tag{2}$$

Equation (2) indicates that the Euclidean distance between each vertex of A and its corresponding closest vertex from B is added to constitute the final distance between the FB domain A and the FB domain B. Equation (2) is employed to calculate the distance between each pair of FB domains that eventually constructs a square matrix giving all dissimilarities of the FB domains in the studied dataset. The k-medoids clustering algorithm is then applied to this calculated distance matrix. It is a partitional clustering algorithm, which structures the input space by assigning each object to the cluster with the closest medoid.

2) Correlation: The second stage of this two-step methodology is the correlation study (i.e., the focus of the first contribution of this paper, discussed in Section 3). The correlation analysis aims to find a mapping between the partitioned FB domains and the explanatory variables affecting the FB domains. A typical FB domain is a function of several factors of different importance. The objective is to carry out the correlation study with the most important factors. The FB domain clusters are correlated with the load demand in France and wind power production in Germany since they are found to be the two most relevant factors [13,14,18], as follows.

Firstly, the data relating to the electricity demand in France and wind power production in Germany over the period that corresponds to the studied FB domains are collected. Then, high, medium, and low thresholds are defined for the collected data corresponding to the respective 33rd, 66th, and 99th percentiles of the load demand data in France and wind power production data in Germany. Afterwards, the probability of occurrence of each FB cluster for each combination of high, medium, and low thresholds of the two selected explanatory variables is calculated. Finally, in the adequacy study, depending on the magnitude of these selected explanatory variables in each generated Monte Carlo sample, the medoid of the cluster with the highest probability is employed, and the linear constraints (shown e.g., in (1)) encoded by that medoid are incorporated into the optimization problem of the adequacy assessment.

Table 1 presents an example of the correlation study results performed on the hourly FB domains by the Belgian TSO (Elia) over a period of one year while having 3 clusters [18]. The results given in Table 1 imply e.g., 58% of the objects (FB domains) placed in the cluster 1 are linked to the conditions where the load demand in France is high and the wind power production in Germany is low. Therefore, the FB domain that is the representative of the cluster number 1 (i.e., its respective

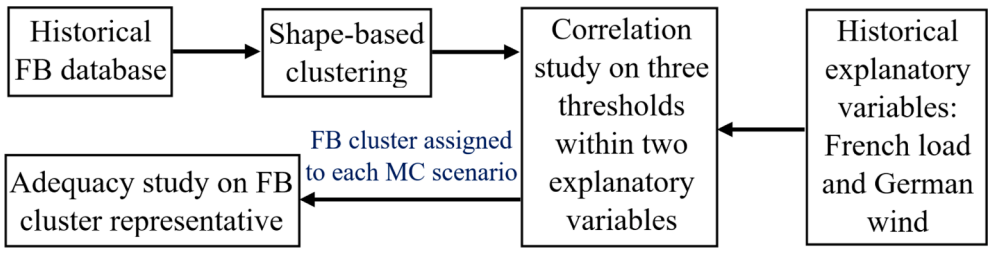

Fig. 2. Illustration of the two-step clustering-correlation methodology employed by the TSOs.

Table 1
Example of the correlation study results with three clusters [18].

		German Wind		
		High	**Medium**	**Low**
French Load	**High**	(0.12, 0.69, 0.19)	(0.45, 0.27, 0.27)	(0.58, 0.18, 0.24)
	Medium	(0.24, 0.53, 0.24)	(0.48, 0.24, 0.27)	(0.67, 0.08, 0.24)
	Low	(0.32, 0.25, 0.43)	(0.43, 0.15, 0.43)	(0.47, 0.11, 0.42)

(x, y, z) gives the probability that cluster no. (1, 2, 3) correlates with a specific combination of the two selected explanatory variables (French load and German wind).

medoid) is employed for adequacy assessments of all Monte Carlo samples within the combination of high French load and low German wind as the cluster number 1 presents the highest correlation (probability) with the latter conditions (combination).

3. Proposed supervised learning-based model relying on the pre-clustered FB domains (two-step methodology)

The correlation study developed by the TSOs characterizes the FB clusters with two selected variables (i.e., load demand in France and wind power generation in Germany) having high, medium, and low thresholds. Such an analysis entails two main shortcomings. First, due to the wide ranges of these three initially selected thresholds, the FB domains with various characteristics may be linked to each combination of those selected variables, which would lead to a poor representation of cross-border exchange capacities in the subsequent adequacy study. Second, the correlation study considering two explanatory variables disregards important information, dependencies, and trends contained in other relevant variables. Consequently, the correlation study would induce modeling inaccuracies in subsequent adequacy assessments. As shown in Table 1, none of the three obtained clusters are strongly correlated with any specific combination of the selected explanatory variables. For instance, when the French load is low and German wind is high (or medium), the maximum probability that a cluster correlates with the latter combination does not exceed 43%.

The introduced shortcomings of the correlation study can be particularly exacerbated when new zones join the FBMC as it requires incorporating several additional input variables. Indeed, increasing the (number of) explanatory variables of the correlation study leads to numerous possible combinations that render the correlation analysis more complex and hardly interpretable. To make it more vivid, two considered explanatory variables having three predefined thresholds lead to 9 possible combinations in the correlation study (as it can be seen in Table 1) while adding a single (new) explanatory variable will triple the number of possible combinations.

A novel supervised learning-based model is proposed in this section that aims at addressing the accuracy and scalability issues of the correlation study utilized by the TSOs. The proposed model does not rely on any initial feature scaling or division of the selected explanatory variables (that can be seen as hyper-parameters affecting the outcomes of the study). Furthermore, it is highly scalable to the number of explanatory variables received as input (dimensionality of the input space) that is essential to fully explore the complex relations present between the input–output spaces.

The proposed supervised learning-based model is applied to the output of the clustering analysis that gives a label to each FB domain in the dataset. The supervised learning task is formulated as a classification problem that aims to define the right FB domain label (class) based on the available explanatory variables. The relationship between the explanatory variables and the FB labels is learned on the historical dataset during the training phase of the supervised learning task.

In a general form, a classification problem can be mathematically expressed as finding the optimal setting of the classifier parameters θ so that the loss function L can be minimized over the training set ($p \in P$):

$$\min_{\theta} \sum_{p \in P} L\left(\underbrace{f_\theta(x_p, p)}_{\widehat{y}_p}, y_p \right) \tag{3}$$

where y_p and $\widehat{y}_p$ are respectively the correct and predicted classes over the training step while P includes the time steps of the training phase. The function f_θ performs the mapping between input x_p and output $\widehat{y}_p$, and L is the loss function, which quantifies the classification accuracy. Once the training phase is completed and the optimal setting of classifier parameters (θ) is obtained, the trained classifier f_θ can be employed to predict the class (label) $\widehat{y}_q$ that corresponds to each new unseen sample of input x_q (where q represents an index of the test set Q).

In this paper, we consider the aggregated hourly load and generation data in each zone of the CWE electricity system as the explanatory variables of the supervised learning process. This choice is adopted given (i) the aggregated zonal load and generation data are relevant to the overall status of each CWE zone being importer or exporter, (ii) these selected variables are (one of) the main inputs of the FB domain calculation process, and (iii) they are the most detailed data publicly available from the FBMC in CWE electricity system. Therefore, our proposed supervised learner model receives during the training phase as the input (x_p), the hourly zonal load and generation data (= 10 inputs for 5 CWE zones) while having the true label y_p (i.e., the cluster representative number) associated with each hourly data from the clustering analysis.

The proposed supervised learning-based framework (within the two-step set-up) is tested employing three classification algorithms, namely Random Forest (RF), K-Nearest Neighbors (KNN), and Support Vector Machine (SVM), presented below. Although other typical classification methods found in the literature could be readily integrated into the proposed framework, these three selected classifiers having different working principles and generalization capabilities will provide a thorough performance evaluation of the proposed framework in comparison with the classical correlation study utilized by the TSOs. It is worth noting that the latter study aims to demonstrate the performance of the proposed supervised learning-based model (for the two-step set-up) in comparison with the classical correlation-based method utilized by the TSOs and not to define the best classification algorithm to be integrated

into the proposed model.

Fig. 3 demonstrates how the proposed supervised learning-based model performs the FB domain assignment task (relying on the clustering analysis results) for the subsequent adequacy assessments.

3.1. Random Forest (RF)

Random forest is an ensemble method that consists of several (i.e., a forest of) decision trees. A decision tree creates a tree-like graph via a set of if-then logical conditions to extract the hidden relationships between input and output spaces of the dataset at hand. Building a decision tree is a recursive process going from the properties of the input spaces to the decision about the associated classes. Starting from a root node that represents a variable (feature) of the input space, it splits into sub-nodes according to a defined rule (e.g., based on the Gini index [28]). The newly generated nodes can represent other features of the input space. They also split into new nodes based on a relevant if-then logical condition. This division procedure purifies the relations between input and output spaces. A decision tree is constructed when all the generated nodes are leaf nodes, where an input feature is explicitly linked to a class of the output space (no more if-then conditions).

RF trains several decision trees in parallel on different subsets of the training dataset considering various subsets of available features (known as bootstrapping task) [30]. The latter ensures that each individual decision tree in the RF model is unique, which can reduce the overall variance of the RF classifier. The final decision of the RF classifier is made by aggregating the decisions of individual trees that helps it to exhibit a good generalization capability. Within its training phase, the RF algorithm aims at defining the right features in each tree to grow and the optimal split of the selected features so that the loss function L can be minimized according to (3). The parameters that need to be selected to optimize the performance of the RF classifier are the number of trees to grow and number of input features (variables) considered in each split.

3.2. K-Nearest Neighbors (KNN)

The traditional supervised learning techniques, such as tree-based methods map a fixed-dimensional input to a fixed-dimensional output. In contrast, the KNN algorithm only focuses on similarities within the input space. In order to determine the class (output) to be assigned to each new observation (input), the KNN finds the K most similar observations from the training set to that new observation according to a selected distance measure. The dominant class associating with the K (nearest) identified observations defines the class of the new observation.

Let assume a dataset where X is a matrix of input features from an observation and Y is a class label. To define the class to be assigned to a given test observation x_q, the KNN firstly determines the K (positive integer) observations closest to x_q, represented by Z. It then estimates the conditional probability for class j as the fraction of points in Z whose response values equal j, as follows [31]:

$$PR\left(Y=j|X=x_q\right)=\frac{1}{K}\sum_{z\in Z}I\left(y_z=j\right) \tag{4}$$

where $I(y_z=j)$ is an indicator variable that equals 1 if the observation z belongs to the class j, and 0 if the class of observation z (y_z) is not identical to the class j. Finally, the class with the highest probability (calculated by (4)) is attributed to the test observation x_q. The KNN is a straightforward method to implement. It requires selecting the number of the considered nearest neighbors (K) and a distance measure to evaluate the dissimilarity between the observations. The choice of these settings can affect the performance of the KNN algorithm.

3.3. Support Vector Machine (SVM)

Support vector machine aims to determine a hyperplane that can separate the data points at hand for a classification task. In a D-dimensional space, a hyperplane is a flat affine subspace of dimension $D-1$. Let assume a set of lp $(=|P|)$ training observations $x_1, x_2, \cdots, x_{lp}$ associating with labels $y_1, y_2, \cdots, y_{lp} \in \{-1, 1\}$. The support vector machine aims at finding the hyperplane $\beta_0+\beta_1X_1+\beta_2X_2+\cdots+\beta_DX_D$ that maximizes the margin M via the following optimization problem [31]:

$$\max_{\beta_0,\beta_1,\cdots,\beta_D,\epsilon_1,\cdots,\epsilon_{lp},M} M \tag{5}$$

$$y_p\left(\beta_0+\beta_1x_{p1}+\beta_2x_{p2}+\cdots+\beta_{pD}x_{pD}\right)\geq M\left(1-\epsilon_p\right)\ \forall p=1,2,\cdots,lp \tag{6}$$

$$\sum_{p=1}^{lp}\epsilon_p\leq C \tag{7}$$

where M refers to the width of the margin separating the training observations. Within the above optimization problem, constraint (6) imposes the data point x_p to be on the correct side of the hyperplane. Given that the training observations are generally not fully separable, the (non-negative) slack variable ϵ_p is introduced to allow an individual observation to be on the wrong side of the hyperplane. Precisely, when $\epsilon_p=0$, the observation x_p lies on the correct side of the hyperplane, $\epsilon_p>0$ indicates that x_p is on the margin M while $\epsilon_p>1$ implies that the observation is placed on the wrong side of the hyperplane. The parameter C is introduced in (7) to limit the total amount of relaxation of constraint (6). In practice, C is treated as a tuning parameter that can control the bias-variance trade-off of the SVM [31]. Although the above principle is stated for a classification problem with two classes $\in\{-1, 1\}$, it can also be extended for the number of classes greater than two ($K_C>2$). One possible way to do so is the one-versus-all approach wherein we train K_C SVM, each time comparing one class against other K_C-1 classes [31].

The SVM is usually combined with a kernel function that maps the input features into a higher dimensional space, which allows to efficiently handle complex classification problems. The most commonly used kernels are the linear, radial, polynomial, and sigmoidal functions, as described in [32]. The choice of an appropriate kernel function and

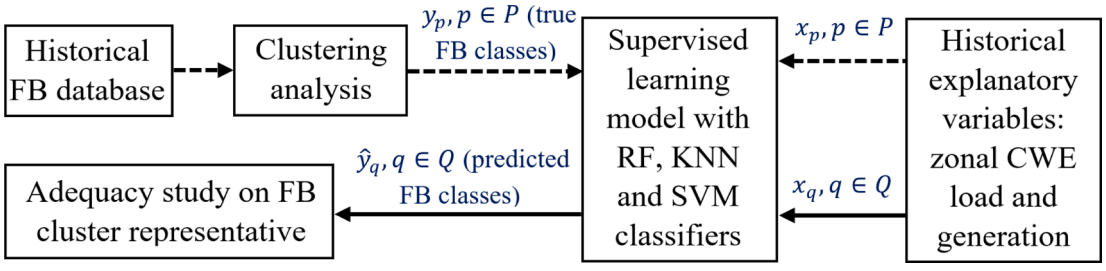

Fig. 3. Illustration of the proposed supervised learning-based model relying on the pre-clustered FB domains within the two-step set-up. P and Q denote sets of time steps of the training and test phases, respectively. Dash (or solid) arrows demonstrate the data flow associated with the training (or test) phase.

proper tuning of its parameters as well as an optimal adjustment of parameter C is essential for an acceptable performance of the SVM classifier.

4. Proposed direct supervised learning-based model (single-step approach)

The classical two-step methodology employed by the TSOs (presented in Section 2.2) induces inaccuracies in adequacy assessments, which are originated from both clustering and correlation analyses. Although the performance of such a two-step approach can be enhanced by leveraging a clustering technique tailored to adequacy assessments (as studied in [19]) and through an improved mapping between explanatory variables and clustered FB data (as targeted in Section 3 of the current paper), the intra-cluster discrepancies may remain significant owing to various shapes and forms of FB domains, which would lead to inevitable modeling inaccuracies in adequacy studies. As a result, the application of FB cluster representatives in adequacy assessments may lead to erroneous outcomes. In order to tackle the latter issue, in this section, we leverage the supervised learning to develop an innovative single-step model that directly maps the selected explanatory variables to the FB domains, without relying on the clustering analysis.

Along the direct mapping process, the initial shapes of FB domains must be preserved as they reflect the grid-feasible exchanges of the considered zones. The proposed single-step model is formulated as a classification problem in which each FB domain in the historical dataset constitutes a unique class. In other words, since within the direct mapping process, the intermediate step (the clustering analysis) is eliminated, the number of available classes equals the number of FB domains in the dataset, which renders the classification task substantially more complex. Consequently, the traditional classification techniques (e.g., tree-based algorithms) that aim to define a link between input and output spaces cannot be employed in the single-step model as it involves numerous classes (i.e., one class per each FB domain in dataset). To address the latter challenge, in this section, we adopt the KNN algorithm (described in Section 3.2), which only focuses on the similarities within the input space that includes noticeably fewer dimensions. To ensure that the proposed single-step KNN-based model does not modify the original shapes of FB domains, we opt here for the (first) nearest neighbor to each observation ($K = 1$).

Overall, our proposed direct classification model is based on the KNN algorithm that identifies the most similar FB domain historically observed to each new (unseen) sample of probabilistic adequacy assessments. The selected explanatory variables (inputs) of the single-step model are the aggregated zonal load and generation in each zone of the CWE, as explained in Section 3. Fig. 4 demonstrates an overview of the working procedure as well as the required inputs of the proposed single-step model for integrating the FB domains into adequacy assessments.

The salient features of the direct supervised learning-based model are threefold. First, thanks to the removal of the clustering phase, the accuracy of subsequent adequacy assessments can be noticeably enhanced (further investigated in Section 4 and demonstrated in Tables 4-6). Second, from the perspective of eliminating the clustering step, the proposed single-step model can considerably lower the computational complexity of the two-step methodology since it does not require performing the time-consuming calculation of distances between FB domains (further discussed in Section 7). Third, the proposed single-step model using the KNN classifier entails no hyper-parameters. Consequently, the performance of the proposed direct model does not depend on any parameter setting, unlike the classical two-step methodology wherein the hyper-parameters such as the selected number of clusters or the defined thresholds for correlation study can significantly affect the final adequacy outcomes (as shown in Tables 5 and 6).

5. Validation in the context of adequacy assessments

In this paper, the cross-validation technique (introduced in Section 5.1) is employed to extend the test phase of the studied methods (presented in Section 5.2 and Table 2) to the whole available database. We assess the performance of each studied method in the context of the

Table 2
Presentation of the studied test cases.

Case no.	Studied test case	Modeling details		Impact on adequacy assessment via (13)
		Clustering technique	Mapping between input–output spaces	
1	Direct KNN classification (single-step method)	NA	KNN classification	Predicted FB domain
2	SB clustering-correlation	SB	Correlation	Predicted cluster representative
3	SB clustering-classification with RF	SB	RF classification	Predicted cluster representative
4	SB clustering-classification with KNN	SB	KNN classification	Predicted cluster representative
5	SB clustering-classification with SVM	SB	SVM classification	Predicted cluster representative
6	SB clustering, no mapping	SB	NA	True cluster representative
7	GO clustering-correlation	GO	Correlation	Predicted cluster representative
8	GO clustering-classification with RF	GO	RF classification	Predicted cluster representative
9	GO clustering-classification with KNN	GO	KNN classification	Predicted cluster representative
10	GO clustering-classification with SVM	GO	SVM classification	Predicted cluster representative
11	GO clustering, no mapping	GO	NA	True cluster representative

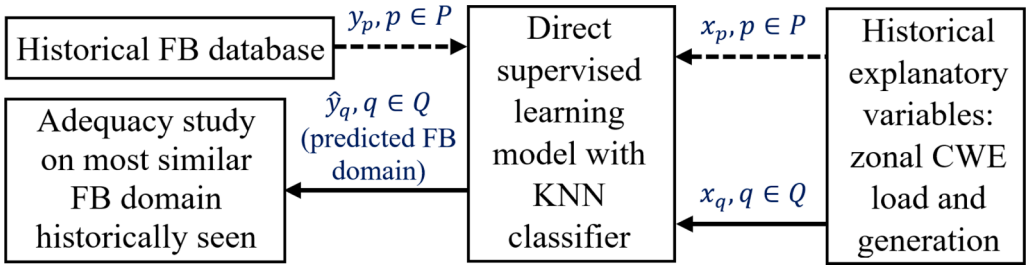

Fig. 4. Illustration of the proposed single-step supervised learning-based model. P and Q denote sets of time steps of the training and test phases, respectively. Dash (or solid) arrows demonstrate the data flow associated with the training (or test) phase.

adequacy study (formulated in Section 5.3) and evaluate the accuracy of obtained results with respect to the considered reference case (ground truth) described in Section 5.4.

5.1. Cross-validation

Traditional practice in the machine learning field consists in training a model with a (bigger) portion of the dataset at hand while utilizing the remaining unseen part of the dataset to test the performance of the trained model, as implemented e.g., in [28,33]. In this paper, we employ the k-fold cross-validation technique and embed it in the context of an adequacy study in order to extend the test phase (validation) of the developed models to the whole available database. The cross-validation based on the k-fold technique splits the dataset to k subgroups. The developed model is trained on $k-1$ groups while it is tested on the remaining subgroup. This procedure is repeated k times while the subsets selected for training and test are consecutively changed [31]. In this work, we consider 5 folds ($k=5$) in the cross-validation procedure. It implies that within each iteration of the cross-validation, 80% of the dataset is reserved for the training while the remaining 20% is employed for the test.

5.2. Test case

The performance of the proposed single-step model presented in Section 4 (i.e., case 1 in Table 2) is benchmarked against various combinations of two-step set-up relying on the goal-oriented (presented in [19]) or shape-based clustering analysis combined with the correlation or classification (proposed in Section 3) study. The studied test cases are presented in Table 2 (where NA indicates a specific analysis is not applied).

These considered test cases permit us (i) to compare and evaluate the performance of each individual model within the two-step methodology, and (ii) to identify the best approach for modeling of the FB domains in adequacy assessments. Particularly, the comparison between cases 2 to 5, which all rely on the same clustering approach (i.e., shape-based), but using different mapping models based on the correlation study (case 2) or the proposed supervised learning-based framework employing RF, KNN and SVM classifiers (cases 3 to 5) demonstrates the performance of the different studied classification methods compared to that of the classical correlation approach used by the TSOs. The latter findings can be also derived from the comparison of cases 7 to 10 since these test cases employ the goal-oriented clustering approach but with different mapping models. Furthermore, by comparing cases 2 and 7 (or cases 3 and 8, or cases 4 and 9, or cases 5 and 10), one can find the impact of clustering the FB domains using the shape-based and goal-oriented distance measures as those mentioned test cases rely on an identical mapping model applied to different clustering approaches. The latter outcome can be fully confirmed by comparing cases 6 and 11 where the shape-based and goal-oriented clustering approaches are solely employed (without mapping). Finally, an overall comparison among the 11 studied test cases can reveal the most accurate FB domain modeling approach for the adequacy assessments.

It should be noted that the test cases 6 and 11 represent a theoretical benchmark, as such a model with only clustering study cannot be utilized in the context of probabilistic adequacy assessments since it does not incorporate any mapping of explanatory variables to FB cluster representatives (through correlation or classification study). Cases 6 and 11 are considered here as they demonstrate the error that directly originates from the clustering part when the mapping error (from the correlation or classification model) is disregarded.

5.3. Economic dispatch calculation for the adequacy assessments

The economic dispatch formulation developed in [19] is used to perform the adequacy assessments on the studied cases given in Table 2. Relying on a linear optimization formulation, the economic dispatch tool aims at minimizing the Energy Not Served (ENS) in the CWE electric system subject to the zonal match of load-generation as well as the available cross-zonal exchange capacities defined by the FB domain, as follows.

$$\underset{G_i, ENS_i}{\text{Min}} \sum_{i=1}^{N} ENS_i \tag{8}$$

$$G_i - LD_i - NP_i + ENS_i = 0 \ \forall i \in N \tag{9}$$

$$\sum_{i=1}^{N} NP_i = 0 \tag{10}$$

$$0 \leq G_i \leq G_i^{max} \tag{11}$$

$$0 \leq ENS_i \tag{12}$$

$$PTDF \times NP \leq RAM \tag{13}$$

where N is the number of zones (countries) participating in the FBMC ($N=5$),G_i denotes the aggregated generation of zone i, LD_i gives the load demand in zone i, and NP_i stands for the net position of zone i (=export − import). The decision variables of the optimization problem (8)-(13) are the zonal ENS (ENS_i) as well as the generation in each zone (G_i). The objective of minimizing the total ENS is given in (8). Equation (9) implies that the generation in each zone must equal the sum of load demand and net power exchanges of that zone. To guarantee the feasibility of the problem at each studied time step, a slack variable i.e.,ENS_i is added to (9) to cover the possible generation shortage of each zone. It is employed only when intra-zonal generation combined with the power exchanges via interconnections cannot cover the zonal load demands. Equation (10) expresses that the sum of zonal net positions must be equal to zero. It implies that the energy exchanges outside the CWE region are not considered here since these exchanges are not defined by the FB domains. Constraint (11) considers the upper and lower bounds on the zonal generations, while constraint (12) defines that the ENS is limited to non-negative values. Lastly, the system of linear constraints (13) incorporates the FB domain identified according to each of the 11 studied cases. Table 2 (last column) represents how the FB domain is identified in each studied test case to be integrated into adequacy assessments via (13).

The presented optimization problem is solved for each time step (hour) of the studied horizon (introduced in Section 6) considering its associated hourly available zonal generations and load demands as well as the FB domain identified (for each hour) according to the studied test case. Given that the focus of this paper is on the modeling of the cross-border exchange capacities via FB domains, the employed adequacy formulation and its inputs are identical in all studied test cases as well as in the reference case (introduced in Section 5.4). The only difference is that the FB domains are integrated via different approaches in the system of linear constraint (13). Once the adequacy assessment is performed over the studied time horizon, the following selected adequacy metrics are calculated, namely the Loss of Load Probability (LOLP) in % and the Total Energy Not Served (TENS) in GWh. The $LOLP_i$ gives the number of non-zero instances of the slack variable in zone i (ENS_i) divided by the total time steps of the studied horizon. The $TENS_i$ equals the sum of ENS_i over the studied horizon.

5.4. Reference adequacy results

Relying on real FBMC data enables us to establish our reference case where the exact hourly FB domain available in the historical database is employed in the hourly adequacy assessment (8)-(13), as depicted in Fig. 5. The exact hourly FB domain is computed for each time step, based on the grid topology and data, considering the network state (load

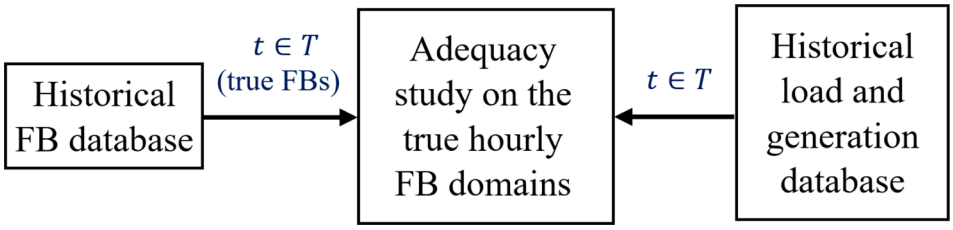

Fig. 5. Illustration of the procedure to determine the true adequacy metrics in the reference case. T denotes the set of all time steps in the database.

demands and generation profiles). Therefore, in the reference case, there is no prediction of FB domain via the single-step or two-step set-up as the exact hourly FB domain calculated beforehand is considered in the hourly adequacy assessments. The adequacy metrics calculated over the studied horizon in this reference case constitute our "true" adequacy outcomes.

The accuracy of adequacy outcomes (metrics) obtained in each considered test case (introduced in Table 2) is evaluated with respect to the true adequacy metrics calculated in the reference case. To do so, the absolute error (difference) between zonal adequacy indicators obtained by each studied test case and the reference case is added up and calculated as follows.

$$\Delta_{LOLP} = \sum_{i=1}^{N} \left| (LOLP_i^{TC} - LOLP_i^{Ref}) \right| \tag{14}$$

$$\Delta_{TENS} = \sum_{i=1}^{N} \left| (TENS_i^{TC} - TENS_i^{Ref}) \right| \tag{15}$$

where $LOLP_i^{TC}$ gives the LOLP indicator in zone i obtained by each of the 11 studied test cases, and $LOLP_i^{Ref}$ presents the LOLP in zone i in the reference case. $TENS_i^{TC}$ and $TENS_i^{Ref}$ denote the TENS index in zone i in the test case (i.e., one of the cases 1 to 11) and the reference case, respectively.

6. Simulation results

The simulations and analyses of this section are carried out on real FB data consisting of hourly FB domains as well as their corresponding hourly aggregated load and generation in each CWE zone. The considered dataset covers the period from January to November 2020 [20]. The data processing as well as the clustering, correlation, and classification analyses are conducted in the R environment while the adequacy assessments are performed in Matlab. The clustering step is carried out using the fast k-medoids algorithm introduced in [37] that has shown a superior performance compared to the classical k-medoids method in [38].

The adequacy evaluation is conducted on the test cases presented in Table 2. Since the performance in cases 2 to 11 depends on the selected number of clusters (n), we perform the adequacy assessments on the latter cases for different numbers of clusters ranging from 2 to 10. When the KNN-based classification within the two-step set-up is employed (in case 4 and case 9), the five nearest neighbors to each observation are considered ($K = 5$) for the classification study. This setting can enhance the overall performance of the KNN classification according to our conducted exploration and experiment. The Euclidean distance is adopted as the employed dissimilarity measure to find the K nearest objects in the KNN algorithm (within both single- and two-step set-ups). Regarding the hyper-parameters of the RF algorithm, the standard parameters introduced in [34] are adopted (the total number of trees to grow equals 500, the number of variables considered at each split is equal to the square root of the number of selected explanatory variables, etc.). For the SVM, the radial kernel function with $C = 100$ is used as it could improve the overall performance of the latter algorithm, based on our conducted experiment. Other selected hyper-parameters of the SVM are identical to the initial settings defined in the employed library [35].

Table 3 gives the true adequacy indices obtained in the reference case for five CWE zones, namely Belgium (BE), Germany (DE), France (FR), Austria (AU), and the Netherlands (NL). Table 4 presents the errors in adequacy indices (calculated by (14) and (15)) when the proposed direct supervised learning-based model (case 1) performs the FB domain assignment task. Tables 5 and 6 demonstrate the errors in LOLP and TENS obtained in cases 2 to 11 while changing the number of clusters from 2 to 10. For a better distinction, the best result (smallest error) obtained in each test case in Tables 5 and 6 is shown in bold.

The main observations in Tables 3-6 are fourfold:

Observation 1: The proposed single-step supervised learning-based approach (case 1) outperforms all other studied test cases. The single-step KNN-based model decreases the errors in LOLP and TENS to 0.73 Percentage Point (PP) and 50.7 GWh, respectively, as can be seen in Table 4. Considering the smallest adequacy errors obtained by the two-step SB clustering-correlation approach (case 2, i.e., the methodology employed by the TSOs) given in Tables 5 and 6 (Δ_{LOLP} = 3.26 PP and Δ_{TENS} = 586 GWh), the proposed direct classification model (case 1) reduces these errors by factors equal to 4.5 (=3.26/0.73) for LOLP, and 11.5 (=586/50.7) for TENS indices. These improvement factors are equal to 1.7 (=1.25/0.73) for LOLP and 6.8 (=345/50.7) for TENS with respect to the best result obtained by the enhanced two-step methodology based on the goal-oriented clustering combined with the proposed supervised learning model employing the SVM classifier (case 10). Furthermore, taking into account the reference adequacy results given in Table 3 having overall (sum of all zones) LOLP and TENS equal to 29.27% and 2867 GWh, the proposed single-step model leads to the normalized errors equal to 2.5% (=0.73/29.27) for LOLP and 1.77% (=50.7/2867) for TENS, which clearly demonstrate the promising performance of the single-step model.

Observation 2: The proposed supervised learning-based model enhances the mapping between the selected explanatory variables and the FB domain cluster representatives (within the two-step set-up). In Tables 5 and 6, one can notice that for each given number of clusters, the results of case 3 (SB clustering-classification with RF), case 4 (SB clustering-classification with KNN), and case 5 (SB clustering-classification with SVM) are close to the outcomes of case 6 (SB clustering with no mapping). Precisely, the gaps between the results of SB clustering with no mapping (case 6) and SB clustering-classification with KNN, RF and SVM (cases 3 to 5) do not exceed 0.26 (=5.16–4.9) PP for LOLP (found with $n = 7$) and 24 (=833–809) GWh for TENS (found with $n = 7$). This implies that minor errors are originated in adequacy outcomes from the proposed supervised learning-based approach (within the two-step set-up) employing RF, KNN, and SVM classification algorithms. The latter finding can also be derived from the comparison of cases 8 to 10 (where the proposed supervised learning-based model

Table 3
Adequacy indices in the reference case.

	BE	DE	FR	AU	NL
LOLP [%]	5.1	12.25	4.33	2.34	5.25
TENS [GWh]	245	1732.8	484.1	125.4	280.2

Table 4
Δ_{LOLP} and Δ_{TENS} Obtained using the single-step model (case 1).

Case no.	Considered model	Δ_{LOLP} [Percentage Point]	Δ_{TENS} [GWh]
1	Direct KNN classification	0.73	50.7

using the KNN, RF and SVM algorithms is tested on the pre-clustered FB domains based on the goal-oriented technique) with case 11 (where the goal-oriented clustering is tested with no mapping part). While the overall performance of the three studied classification algorithms remains similar for various numbers of clusters, one can notice that the SVM classifier employed in cases 5 and 10 leads to the smallest errors in Tables 5 and 6 (compare the bold values).

Observation 3: The correlation study employed by the TSOs poorly maps the selected explanatory variables to the clustered FB domain representatives. In Tables 5 and 6, it is seen that the correlation model used in case 2 (or case 7) deviates the results obtained by the stand-alone clustering analysis with no mapping step in case 6 (or case 11). For instance, comparison of results of cases 7 and 11 in Table 5 demonstrates that the correlation model applied to the goal-oriented clustering (i.e., case 7) increases the initial errors of the goal-oriented clustering with no mapping part (given in case 11) from 1.5 to 4.57 PP for $n = 8$, from 2.82 to 4.69 PP for $n = 9$, and from 2 to 3.61 PP for $n = 10$. Similarly, in case 2 (shape-based clustering-correlation), the correlation model affects the results of case 6 (i.e., shape-based clustering with no mapping), for $n > 3$, as the number of clusters increases. As it can be seen in Tables 5 and 6, these variations (representing the errors linked to the correlation study) are in both positive and negative directions.

Observation 4: The performance of the two-step set-ups depends on the selected number of clusters (n). Particularly, in Tables 5 and 6, one can observe that the stand-alone goal-oriented clustering method in case 11 starts with high errors ($\Delta_{LOLP} = 7.87$ PP and$\Delta_{TENS} = 1183$ GWh) for $n = 2$. These errors are then reduced by increasing the number of clusters (to $n > 3$), where with $n = 8$, Δ_{LOLP} and Δ_{TENS} reach 1.5 PP and 388 GWh, respectively. The stand-alone shape-based clustering approach without mapping part (case 6) is less sensitive to the choice of n since by changing the number of clusters, Δ_{LOLP} remains between 4.9 and 5.2 PP and Δ_{TENS} varies between 801 and 819 GWh, which are bigger than the best results obtained by case 11 (stand-alone goal-oriented clustering). The improved accuracy of the goal-oriented clustering method compared to the shape-based clustering technique has been discussed in [19].

7. Discussion

Observation 1 states that the single-step model results in the smallest errors in adequacy studies. The superior performance of the proposed direct model is achieved thanks to eliminating the clustering step and capturing the temporal similarities present in FB data. Indeed, it exists an inherent temporal similarity among the hourly FB domains as a similar load demands and generation profiles in a given network topology would lead to FB domains with similar characteristics. The proposed single-step method based on the KNN algorithm captures this temporal similarity by defining the nearest neighbor (K = 1) to each working state in the adequacy study and assigns its FB domain, known from the historical database to the working state at hand. The two-step set-up however tries to find the cluster representative that better matches with each working state in the adequacy study. Given that the hourly FB domains take numerous shapes and forms, a cluster representative cannot truly capture the physical properties contained in all FB domains within the cluster. Consequently, the application of cluster representative in adequacy assessment leads to erroneous outcomes. The latter issue can be partly addressed by changing the number of clusters and using the goal-oriented distance measure (as shown in test case 11). Nevertheless, some considerable errors originating from the clustering

Table 5
Δ_{LOLP} [percentage point] obtained using cases 2 to 11 for various numbers of clusters.

Case no.	Considered model	*Number of clusters (n)*								
		2	***3***	***4***	***5***	***6***	***7***	***8***	***9***	***10***
2	SB clustering-correlation	4.8	4.84	3.66	**3.26**	3.58	3.65	3.7	6.35	5.75
3	SB clustering- classification with RF	5.15	5.03	4.95	5.01	5.13	5.12	4.88	**4.77**	4.9
4	SB clustering- classification with KNN	4.96	5.12	4.91	4.95	4.92	4.9	5.09	5.03	**4.83**
5	SB clustering- classification with SVM	5.24	5.09	5.07	5.09	5.18	5.18	5.04	**4.77**	4.95
6	SB clustering, no mapping	5.2	5.04	5.03	5.03	5.16	5.16	5.06	**4.9**	4.95
7	GO clustering- correlation	6.71	4.04	4.49	3.48	**3.34**	3.86	4.57	4.69	3.61
8	GO clustering-classification with RF	7.86	7.88	7.7	2.15	2.36	1.8	2	2.4	**1.68**
9	GO clustering-classification with KNN	8.03	8	8	2.42	2.31	1.93	**1.35**	2.22	1.73
10	GO clustering-classification with SVM	8.05	8.15	9	2.34	2.07	1.67	**1.25**	2.4	1.91
11	GO clustering, no mapping	7.87	7.94	8.06	2.48	2.39	1.87	**1.5**	2.82	2

Table 6
Δ_{TENS}[GWh] obtained using cases 2 to 11 for various numbers of clusters.

Case no.	Considered model	*Number of clusters (n)*								
		2	***3***	***4***	***5***	***6***	***7***	***8***	***9***	***10***
2	SB clustering-correlation	859	810	710	670	601	**586**	609	893	680
3	SB clustering- classification with RF	830	831	824	**817**	831	833	824	819	826
4	SB clustering- classification with KNN	830	**809**	816	818	825	829	827	824	823
5	SB clustering- classification with SVM	805	**798**	803	804	805	805	811	806	802
6	SB clustering, no mapping	819	813	808	807	809	809	807	**801**	803
7	GO clustering- correlation	1105	638	729	**566**	576	589	589	739	637
8	GO clustering-classification with RF	1166	1192	1172	415	394	**385**	425	525	448
9	GO clustering-classification with KNN	1122	1272	1211	419	401	396	**393**	474	475
10	GO clustering-classification with SVM	1186	1349	1325	430	350	**345**	390	474	476
11	GO clustering, no mapping	1183	1302	1264	456	433	422	**388**	523	496

analysis remain inevitable. The proposed single-step model directly defines the most similar FB domain historically observed to each new sample of adequacy assessment (without doing a clustering step). As a result, its identified FB domain can closely align with the considered conditions in adequacy assessment, which is not the case when the FB cluster representative (medoid) according to the two-step methodology is integrated into adequacy assessment.

Besides its enhanced modeling accuracy, the proposed single-step model eliminates the computational complexity of the two-step set-up (relating to the pre-processing step of the subsequent adequacy assessments) since it does not require calculating the distance between each pair of FB domains in the historical dataset, which is overly time-consuming when using the shape-based distance measure employed by the TSOs. Such a shape-based distance calculation for 100 5-dimensional FB domains would take around 240 s [19], which implies if we extend the dataset to 8760 hourly FB domains of a typical year, the time needed for the construction of the matrix of distances (8760×8760) would be around 511 h (assuming a linear upscaling). The latter operation would take around 4.2 h using the goal-oriented distance measure developed in [19]. The proposed single-step model can accomplish the FB domain assignment task within the adequacy evaluation in almost real time. Although the proposed single-step model demonstrates a superior performance in terms of modeling accuracy and computational time compared to all studied two-step set-ups, it imposes that the hourly adequacy assessment is performed on a different FB domain for each Monte Carlo scenario. As a result, the commercial software that is used by the TSOs to perform the probabilistic adequacy assessments should be equipped with this possibility to be able to update the FB domain for each Monte Carlo sample. The latter functionality should be embedded, for instance, in the Antares simulator being used by the CWE TSOs [14,29].

Observations 2 and 3 express that within the two-step methodology, the proposed supervised learning-based model outperforms the correlation analysis for mapping the explanatory variables to correct FB clusters. The improved performance of the proposed classification model is rooted in two main reasons. First, the classification study receives more input features, i.e., 10 variables representing the aggregated load and generation in 5 CWE zones, compared to the correlation study that works on the basis of 2 input variables, i.e., load demand in France and power generation in Germany. Having access to these complementary input features would reveal new (multi-variate) dependencies contained in the studied dataset that can provide a better generalization capability to the classification study. Second, the classification analysis does not require any initial feature scaling or discretization of the selected explanatory (input) variables that can lead to high bias errors by linking various FB domains with different characteristics to the same combination of the predefined levels in input variables, which is at the core of the correlation study.

Table 7 presents an overall performance comparison among (i) the classical shape-based clustering-correlation methodology employed by the TSOs, (ii) the proposed supervised learning-based model relying on the clustered FB data (for the two-step approach), and (iii) the proposed single-step model.

8. Conclusion

In this paper, novel data-driven models are proposed to enhance the modeling of FB domains in the European resource adequacy assessments. Following the two-step clustering-correlation methodology employed by the TSOs, we firstly propose a supervised learning-based model to improve the mapping between several relevant explanatory variables and the clustered FB domains. By covering the shortcomings of the correlation study employed by the TSOs, the proposed supervised learning framework can improve the modeling accuracy and scalability of the classical two-step methodology. Additionally, we leverage the supervised learning to develop a single-step model that directly maps the selected explanatory variables to the FB domains, without relying on the clustering analysis. This proposed single-step model defines for each scenario of the probabilistic adequacy assessments, the most similar FB domain historically observed, based on the received explanatory variables using the KNN algorithm.

The simulations conducted in this paper confirm the superior accuracy of the proposed single-step model, which lowers the errors in the LOLP metric by factors equal to 4.5 and 1.7, compared to the best outcomes obtained by the classical clustering-correlation methodology employed by the TSOs and the enhanced two-step approach using the proposed supervised learning model, respectively. Furthermore, by directly mapping the explanatory variables to FB domains, the proposed single-step model eliminates the computationally heavy operation required for the clustering analysis (to calculate the distance between each pair of FB domains in dataset). Consequently, the proposed single-step model can execute the FB domain assignment task in a nearly real-time fashion. Moreover, the proposed single-step model does not require tuning any hyper-parameters while the performance of the two-step methodology heavily depends on the factors such as the selected number of clusters and the predefined thresholds for the correlation analysis.

The current research showcases how a tailored supervised learning model can enhance the accuracy, scalability, and computational complexity of the European resource adequacy assessments. Hence, it contributes to building confidence of the power system operators and power system community in the potential of machine learning to enhance the classical model-based analyses by capturing the complex trends and dynamics contained in emerging datasets of modern power systems, in a data-driven fashion.

CRediT authorship contribution statement

Bashir Bakhshideh Zad: Conceptualization, Methodology,

Table 7
Performance comparison between two-step and single-step set-ups.

	Modeling accuracy	Calculation burden	Hyper-parameter dependency	Scalability	Adaptability with existing commercial software
Classical methodology based on SB clustering-correlation employed by the TSOs (two-step)	Least accurate	Overly heavy using SB clustering	High, i.e., to the selected number of clusters and thresholds for correlation study	Not scalable leading to numerous combinations in correlation study	Adaptable e.g., with Antares simulator
Proposed model using supervised learning relying on clustered FB domains (two-step)	More accurate than classical model using correlation study	Overly heavy using SB, complexity enhanced by GO	High, i.e., to the selected number of clusters and the classifier parameters	Scalable with extension of FB region	Adaptable e.g., with Antares simulator
Proposed single-step model based on supervised learning	Most accurate	Does not exist, the FB assignment task is performed in almost real time	Does not exist, independent of parameter settings	Scalable with extension of FB region	Needs further developments of Antares simulator

Investigation, Software, Validation, Formal analysis, Data curation, Writing – original draft, Writing – review & editing. **Jean-François Toubeau:** Conceptualization, Methodology, Writing – review & editing, Validation. **Kenneth Bruninx:** Conceptualization, Methodology, Writing – review & editing, Validation. **Behzad Vatandoust:** Conceptualization, Methodology, Writing – review & editing, Validation. **Zacharie De Grève:** Conceptualization, Methodology, Writing – review & editing, Validation. **François Vallée:** Conceptualization, Methodology, Writing – review & editing, Validation, Supervision, Project administration.

Declaration of Competing Interest

The authors declare the following financial interests/personal relationships which may be considered as potential competing interests: Bashir Bakhshideh Zad reports financial support was provided by University of Mons.

Acknowledgment

This research was carried out in the context of the ADABEL project, supported by the Energy Transition Fund of the Federal Public Service (FPS) Economy, S.M.E.s, Self-Employed and Energy, Belgium.

References

[1] Billinton R, Karki R, Gao Y, Huang D, Hu P, Wangdee W. Adequacy assessment considerations in wind integrated power systems. IEEE Trans on Power Syst 2012;27(4):2297–305.
[2] Tómasson E, Söder L. Generation adequacy analysis of multi-area power systems with a high share of wind power. IEEE Trans on Power Syst 2018;33(4):3854–62.
[3] Vallée F, Brunieau G, Pirlot M, Deblecker O, Lobry J. Optimal wind clustering methodology for adequacy evaluation in system generation studies using nonsequential Monte Carlo simulation. IEEE Trans on Power Syst 2011;26(4):2173–84.
[4] Cepeda M, Saguan M, Fino D, Pignon V. Generation adequacy and transmission interconnection in regional electricity markets. Energy Policy 2009;37:5612–22.
[5] "Commission regulation (EU) 2015/1222 of 24 July 2015 establishing a guideline on capacity allocation and congestion management," Available: https://eur-lex.europa.eu/legal-content/EN/TXT/?uri=CELEX%3A32015R1222.
[6] Schönheit D, Kenis M, Lorenz L, Möost D, Delarue E, Bruninx K. Toward a fundamental understanding of flow-based market coupling for cross-border electricity trading. Adv Appl Energy 2021;2:100027.
[7] Schönheit D, Weinhold R, Dierstein C. The impact of different strategies for generation shift keys (GSKs) on the flow-based market coupling domain: a model-based analysis of Central Western Europe. Appl Energy 2020;258:114067.
[8] Schönheit D, Bruninx K, Kenis M, Möst D. Improved selection of critical network elements for flow-based market coupling based on congestion patterns. Appl Energy 2022;306:118028.
[9] Finck R. Impact of flow-based market coupling on the European electricity markets. Sustainability Management Forum NachhaltigkeitsManagementForum 2021;29(2):173–86.
[10] Henneaux P, Lamprinakos P, de Maere d'Aertrycke G, Karoui K. Impact assessment of a minimum threshold on cross-zonal capacity in a flow-based market. Electric Power Syst Res 2021;190:106693.
[11] Poplavskaya K, Totschnig G, Leimgruber F, Doorman G, Etienne G, de Vries L. Integration of day-ahead market and redispatch to increase cross-border exchanges in the European electricity market. Appl Energy 2020;278:115669.
[12] "Regulation (EU) 2019/943 of the European Parliament and of the council of 5 June 2019 on the internal market for electricity," Available: https://eur-lex.europa.eu/legal-content/EN/TXT/PDF/?uri=CELEX:32019R0943&from=EN.
[13] "Generation adequacy assessment," Pentalateral Energy Forum, 2018, Available: https://www.benelux.int/files/1615/1749/6861/2018-01-31_-_2nd_PLEF_GAA_report.pdf.
[14] "Modelling of flow-based domains in Antares for adequacy studies," RTE, France, 2017, Available: https://antares-simulator.org/media/files/page/ZHX0N-171024-Rte-Modelling-of-Flow-Based-Domains-in-Antares-for-Adequacy-Studies.pdf.
[15] "Mid-term adequacy forecast, ENTSO-E," 2019, Available: https://eepublicdownloads.entsoe.eu/clean-documents/sdc-documents/MAF/2019/MAF%202019%20Appendix%202%20-%20Methodology.pdf.
[16] "Typical flow-based days selection," RTE, 2017, Available: https://antares-simulator.org/media/files/page/7NY5W-171024-Rte-Typical-Flow-Based-Days-Selection-1.pdf.
[17] "Adequacy study for Belgium: the need for strategic reserve for winter 2020-21," Elia, Belgium, 2019, Available: https://www.elia.be/-/media/project/elia/shared/documents/elia-site/studies/2019/strategic-reserve-for-winter-2020-21.pdf?la=en.
[18] "Adequacy and flexibility study for Belgium 2020-2030," Elia, Belgium 2019, Available: https://www.elia.be/en/electricity-market-and-system/adequacy/adequacy-studies.
[19] Bakhshideh Zad B, Vatandoust B, Toubeau JF, Bruninx K, De Grève Z, Vallée F. Enhanced integration of flow-based market coupling in short-term adequacy assessment. Electr Power Syst Res 2021;201:107507.
[20] Joint allocation office, Market data, Implicit allocation, Available: https://www.jao.eu/implict-allocation.
[21] Sohail Ibrahim M, Dong W, Yang Q. Machine learning driven smart electric power systems: current trends and new perspectives. Appl Energy 2020;272:115237.
[22] Lei X, Yang Z, Yu J, Zhao J, Gao Q, Yu H. Data-driven optimal power flow: a physics-informed machine learning approach. IEEE Trans on Power Syst 2021;36(1):346–54.
[23] Venzke A, Chatzivasileiadis S. Verification of neural network behaviour: formal guarantees for power system applications. IEEE Trans on Smart Grid 2021;12(1):383–97.
[24] Pined S, Morales JM. Is learning for the unit commitment problem a low-hanging fruit? Electr Power Syst Res 2022;207:107851.
[25] Wang Y, Von Krannichfeldt L, Zufferey T, Toubeau JF. 'Short-term nodal voltage forecasting for power distribution grids: An ensemble learning approach'. Appl Energy 2021;304:117880.
[26] Cui W, Zhang B. Lyapunov-regularized reinforcement learning for power system transient stability. IEEE Control Syst Lett 2021;6:974–9.
[27] Dalal G, Gilboa E, Mannor S, Wehenkel L. Chance-constrained outage scheduling using a machine learning proxy. IEEE Trans Power Syst 2019;34(4):2528–40.
[28] Toubeau JF, Pardoen L, Hubert L, Marenne N, Sprooten J, De Grève Z, et al. Machine learning-assisted outage planning for maintenance activities in power systems with renewables. Energy 2022;238:121993.
[29] Doquet M, Fourment C, Roudergues J. Generation & transmission adequacy of large interconnected power systems: a contribution to the renewal of Monte-Carlo approaches, in Proc. 2011 IEEE Madrid PowerTech.
[30] Misra S, Li H. Machine learning for subsurface characterization. Elsevier; 2020. p. 243–87.
[31] James G, Witten D, Hastie T, Tibshirani R. An introduction to statistical learning: with applications in R. Springer; 2013.
[32] Hearst MA, Dumais ST, Osuna E, Platt J, Scholkopf B. Support vector machines. IEEE Intell Syst 1998;13(4):18–28.
[33] Codjo EL, Bakhshideh Zad B, Toubeau JF, François B, Vallée F. Machine learning-based classification of electrical low voltage cable degradation. Energies 2021;14:2852.
[34] Breiman L, Cutler A, Liaw A, Wiener M. Breiman and Cutler's Random Forests for classification and regression. RDocumentation 2022.
[35] Chih-Chung C, Chih-Jen L. LIBSVM: a library for support vector machines.
[36] Vallée F, Versèle C, Lobry J, Moinya F. Non-sequential Monte Carlo simulation tool in order to minimize gaseous pollutants emissions in presence of fluctuating wind power. Renew. Energy 2013;50:317–24. https://doi.org/10.1016/j.renene.2012.06.046.
[37] Park H-S, Jun C-H. A simple and fast algorithm for K-medoids clustering. Expert Syst. Appl. 2009;36(2):3336–41. https://doi.org/10.1016/j.eswa.2008.01.039.
[38] Bakhshideh Zad B, Toubeau J-F, Vatandoust B, Zacharie DG, Vallée F. Advanced clustering of flow-based domains for adequacy study purposes. 2021 IEEE Madrid PowerTech 2021. https://doi.org/10.1109/PowerTech46648.2021.9495023.
[39] Toubeau J-F, Bakhshideh Zad B, Hupez M, De Grève Z, Vallée F. Deep reinforcement learning-based voltage control to deal with model uncertainties in distribution networks. Energies 2020;13(15):3928. https://doi.org/10.3390/en13153928.